Fuzzy stability analysis of regenerative chatter in milling

Neil D Sims[a,*], Graeme Manson[a], Brian Mann[b]

[a]*Department of Mechanical Engineering, The University of Sheffield, Mappin Street, Sheffield, S1 3JD, UK*
[b]*Duke University, Department of Mechanical Engineering and Materials Science, Durham, NC 27708, USA*

Abstract

During machining, unstable self-excited vibrations known as regenerative chatter can occur, causing excessive tool wear or failure, and a poor surface finish on the machined workpiece. Consequently it is desirable to predict, and hence avoid the onset of this instability. Regenerative chatter is a function of empirical cutting coefficients, and the structural dynamics of the machine-tool system. There can be significant uncertainties in the underlying parameters, so the predicted stability limits do not necessarily agree with those found in practice. In the present study, fuzzy arithmetic techniques are applied to the chatter stability problem. It is first shown that techniques based upon interval arithmetic are not suitable for this problem due to the issue of recursiveness. An implementation of fuzzy arithmetic is then developed based upon the work of Hanss and Klimke. The arithmetic is then applied to two techniques for predicting milling chatter stability: the classical approach of Altintas, and the time-finite element method of Mann. It is shown that for some cases careful programming can reduce the computational effort to acceptable levels. The problem of milling chatter uncertainty is then considered within the framework of Ben-Haim's information-gap theory. It is shown that the presented approach can be used to solve process design problems with robustness to the uncertain parameters. The fuzzy stability bounds are then compared to previously published data, to investigate how uncertainty propagation techniques can offer more insight into the accuracy of chatter predictions.

Key words: fuzzy arithmetic, milling chatter, affine arithmetic, interval arithmetic, uncertainty

1. Introduction

Regenerative chatter is a self-excited vibration that can arise in many machining operations. It the most common form of machining chatter [1], and leads to an unacceptable workpiece surface finish, excessive tool wear, and potential damage to the machine itself. Consequently a great deal of research has been performed in order to understand, predict, and prevent regenerative chatter. Although the underlying mechanism is now well understood, the uncertainties that arise during practical machining operations mean that the stability of the actual process does not always match the expected behaviour. For example, chatter stability is strongly dependent upon the structural dynamics of the system (tool, workpiece, and machine), as well as being a function of empirically derived cutting coefficients. Consequently, variations in the structural dynamics (e.g. between nominally identical tools) or variations in cutting properties (e.g. between material batches) can have a dramatic effect on the chatter stability.

Where statistical data is available to describe the variability and uncertainty in parameters, probabilistic techniques (e.g. Monte Carlo simulations) can be applied to the chatter stability problem [2]. However, detailed statistical data are not always available for a number of reasons. For example, identifying the probability distribution of the empirical cutting coefficients would require extensive testing with differing stages of tool wear. The distribution of the modal parameters (or complete frequency response function) for the structural components would also require extensive testing. Even then, it may not be possible to measure the structural behaviour under the required conditions, e.g. tool rotation and pre-load. Consequently, economic and practical issues force the engineer to consider alternative, non-probabilistic techniques that can estimate the chatter stability whilst still accounting for the variability or uncertainty in the process parameters.

One such approach that has been used for various problems in structural dynamics [3, 4] is fuzzy arithmetic. The present article is motivated by the fact that there are have been

---

*Corresponding author
Email addresses: `n.sims@sheffield.ac.uk` (Neil D Sims)
URL: `www.dynamics.group.shef.ac.uk/people/neil` (Neil D Sims)

very few previous contributions that have applied fuzzy arithmetic to regenerative chatter problems. One relevant study is the work of Fansen and Junyi [5], who used fuzzy methods to interpret the onset of stability in experimental machining tests. However, the present contribution is primarily concerned with the prediction of chatter stability, rather than experimental identification methods. The most relevant study is the earlier work of Fansen et al [6], who applied fuzzy arithmetic to the classical regenerative chatter model described by Tlusty [1]. Fuzzy stability lobes were mainly developed for the case of single-degree-of-freedom structural dynamics, with a fuzzy-valued damping ratio. For this case, the classical chatter model can provide an analytical solution where there is only one fuzzy output: the limiting depth of cut at which chatter occurs. The output is very easy to compute and is often monotonic with respect to the fuzzy input. Consequently, Fansen et al. [6] were able to present an analytical expression for the fuzzy output of the system.

The present study includes two key aspects which differ from Fansen et al's work. First, more recent and accurate regenerative chatter models are considered which are specifically focussed on milling. Second, there is no constraint on the fuzziness of the input parameters to the model (i.e. any number of inputs can be fuzzy). This results in model predictions that are bivariate and non-monotonic. In other words, the chatter stability is fuzzy with respect to both depth of cut and spindle speed. This means that the fuzzy equations cannot be directly manipulated or solved, and so novel mathematical techniques or approximations are required.

Similar issues arise with many other engineering modelling techniques that have been investigated using fuzzy methods (e.g. finite element methods [3]). One approach that has been adopted is to consider each fuzzy variable at different 'levels of membership', and to use interval arithmetic to calculate the corresponding model outputs. Alternatively, the response at each membership level can be approximated by performing multiple 'crisp' calculations using standard arithmetic [7]; reassembling the results of these calculations leads to fuzzy number(s) that describe the output to the engineering model. One methodology for implementing this approach is the so-called transformation method [4].

In the present study, fuzzy arithmetic is applied to the chatter stability problem, by

3

adapting two different stability algorithms from the recent literature. The study focuses on milling, since this machining process is particularly susceptible to regenerative chatter, and substantial performance gains can be made if the chatter stability is properly understood.

After introducing two chatter stability models, it is shown that interval arithmetic methods are unsuitable for this problem, due to the recursive nature of the stability models. A 'design of experiments' approach is then adopted, following the work of Hanns [8] and Klimke [9]. Two numerical examples are used to demonstrate the potential advantages of the fuzzy analysis. In the first case, it is shown how concerns over the uncertainty/variability of two process variables can influence the stability boundary. A robust process design is then selected, using the fuzzy approach. In the second case, previously published experimental data is compared to stability prediction models. It is shown that accounting for uncertainty or variability in the process parameters can serve to justify deviations between the experimental and predicted behaviour.

2. Milling stability analysis

During milling, it is desirable to maximise the productivity, or metal removal rate, whilst maintaining acceptable tool wear and avoiding chatter. The metal removal rate M_{rr} is given by:

$$M_{rr} = brw_f \qquad (1)$$

where b is the axial depth of cut, r is the radial immersion of the tool into the workpiece, and w_f is the workpiece feed rate. The feed rate is commonly set to achieve a constant feed per tooth f_{pt} regardless of the spindle speed Ω (rev/min) and number of teeth N_t:

$$w_f = \frac{\Omega f_{pt} N_t}{60} \qquad (2)$$

Meanwhile, self-excited chatter vibrations can arise due to the 'regeneration of surface waviness' [1], which results in a stability lobe diagram such as the one shown schematically in Fig. 1. Here, it can be seen that the chatter stability varies with milling spindle speed and milling axial depth of cut. Contours of constant Ωb are also shown on Fig. 1, to indicate how the metal removal rate M_{rr} varies.
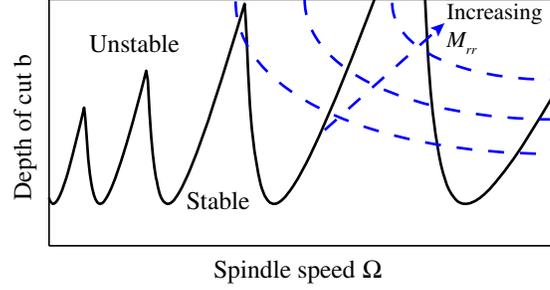
4

Figure 1: Schematic relationship between spindle speed, depth of cut, and stability.

In the present study, two stability analysis methods will be implemented, using fuzzy arithmetic, to determine a fuzzy stability lobe. The methods share the same basic model for the forces and vibrations during milling. This model will now be summarised.

2.1. Forces and deflections

An orthogonal milling scenario is considered in Fig. 2. The tool has N_t teeth and is rotating at a constant angular speed of Ω rev/min, which means that the time delay between one tooth pass and the next is:

$$\tau = \frac{60}{\Omega N_t} \tag{3}$$

Assuming a circular tooth path and a feed per tooth w_f, the chip thickness for tooth j is given by [10, 11, 12]:

$$w_j = g\left(\phi_j\left(t\right)\right) \times$$
$$\left[w_f \sin\left(\phi_j\left(t\right)\right) + \left(u_x\left(t\right) - u_x\left(t - \tau\right)\right) \sin\left(\phi_j\left(t\right)\right) + \left(u_y\left(t\right) - u_y\left(t - \tau\right)\right) \cos\left(\phi_j\left(t\right)\right)\right] \tag{4}$$

where $u_x(t)$ and $u_y(t)$ are the relative vibrations between the tool and workpiece in the x and y directions respectively, and $\phi_j(t)$ is the angle of the tooth as shown in Fig. 2. The function g is a unit step function which has a value unity when tooth j is engaged in the workpiece:

$$g(\phi_j(t)) = \begin{cases} 1 & \text{if } \phi_{st} < \phi_j(t) < \phi_{ex} \\ 0 & \text{if } \phi_{st} > \phi_j(t) \text{ or } \phi_j(t) > \phi_{ex} \end{cases} \tag{5}$$
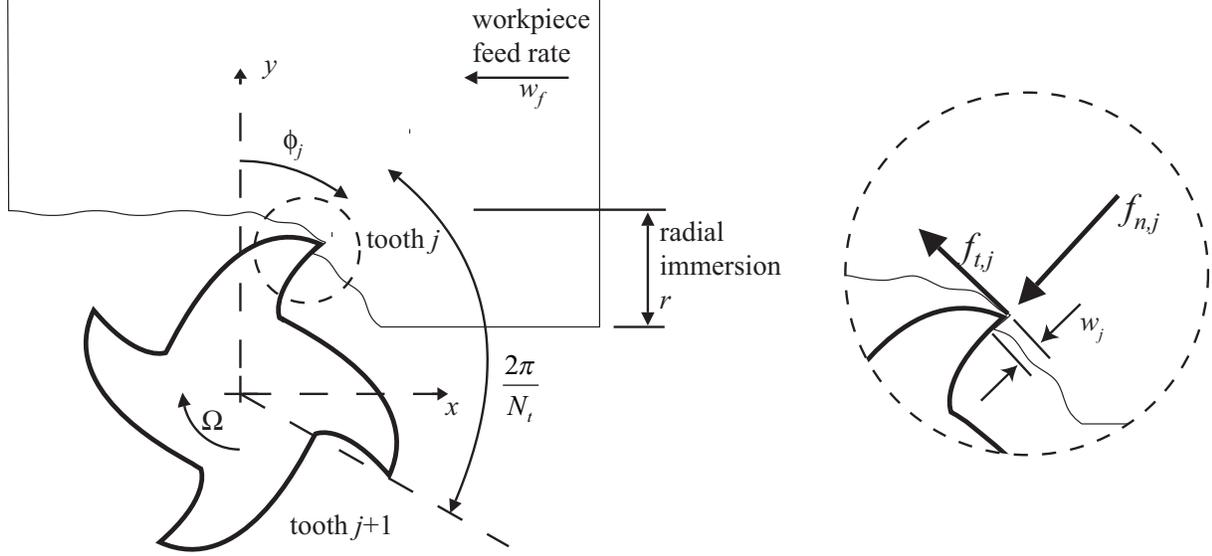
5

Figure 2: Schematic representation of milling.

Here, ϕ_{st} and ϕ_{ex} define the angles at which the teeth enter or exit the workpiece. For a radial immersion r and tool diameter D they become:

$$
\begin{aligned}
\phi_{st} &= \begin{cases} 0 & \text{up milling} \\ \pi - \cos^{-1}\left(1 - 2\frac{r}{D}\right) & \text{down milling} \end{cases} \\
\phi_{ex} &= \begin{cases} \cos^{-1}\left(1 - 2\frac{r}{D}\right) & \text{up milling} \\ \pi & \text{down milling} \end{cases}
\end{aligned}
\tag{6}
$$

Returning to Eq. (4), as with previous literature [10] the static component $w_f \sin(\phi_j)$ is neglected in the stability analysis because it does not contribute to the regenerative effect. Clearly, the chip generation process depends upon the difference between current displacements u_x, u_y, and displacements at previous time points, due to the presence of the delay term τ.

Meanwhile, with reference to Fig. 2 it is often assumed that the forces produced by each tooth j in the cutting process are proportional to the chip thickness w_j and axial depth of cut b, as follows:

$$
\begin{aligned}
f_{t,j} &= K_t b w_j \\
f_{n,j} &= K_r f_{t,j}
\end{aligned}
\tag{7}
$$

6

which leads to corresponding forces in the x and y directions. The empirical cutting force coefficients K_t and K_r can also be expressed as a magnitude K_s and an angle β:

$$\begin{aligned} K_s &= K_t \sqrt{1 + K_r^2} \\ \beta &= \tan^{-1}\left(\frac{1}{K_r}\right) \end{aligned} \tag{8}$$

If the tool is able to vibrate in the x and y directions (due to its structural dynamics), then the forces in Eq. (7) induce vibrations u_x and u_y. This results in a mechanism of self-excited vibration that is illustrated schematically in Fig. 3. The aim, therefore, is for a given spindle speed Ω to predict the depth of cut b_{lim} at which the self-excited vibrations become unstable. This is known as the chatter stability boundary, and the relationship between Ω and b_{lim} is referred to as the stability lobe diagram. In the next sections, two alternative methods for determining the stability lobe diagram are summarised.
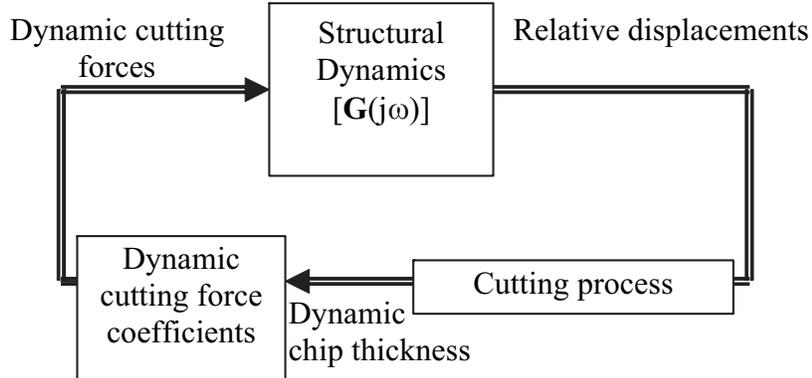

Figure 3: Block diagram of chatter vibration in milling.

2.2. Time-averaged 2DOF chatter stability analysis

Budak and Altintas [13] proposed an analytical method for determining chatter stability in milling. They assumed that the structural dynamics of the tool at the cutting location could be described by two linear frequency response functions (G_{xx}, G_{yy}). They then showed that the relative displacements between tool and workpiece depend upon four periodic milling force coefficients that map the chip thickness to the cutting force. The first term in the Fourier series of these periodic coefficients was then taken, effectively time-averaging

7

the coefficients. The coefficients are given by:

$$
\begin{aligned}
\alpha_{xx} &= \tfrac{1}{2} \left[\cos 2\phi - 2K_r \phi + K_r \sin 2\phi \right]_{\phi_{st}}^{\phi_{ex}} \\
\alpha_{xy} &= \tfrac{1}{2} \left[-\sin 2\phi - 2\phi + K_r \cos 2\phi \right]_{\phi_{st}}^{\phi_{ex}} \\
\alpha_{yx} &= \tfrac{1}{2} \left[-\sin 2\phi + 2\phi + K_r \cos 2\phi \right]_{\phi_{st}}^{\phi_{ex}} \\
\alpha_{yy} &= \tfrac{1}{2} \left[-\cos 2\phi - 2K_r \phi - K_r \sin 2\phi \right]_{\phi_{st}}^{\phi_{ex}}
\end{aligned}
\tag{9}
$$

The characteristic equation of the system can then be written as:

$$
a_0 \Lambda^2 + a_1 \Lambda + 1 = 0
\tag{10}
$$

Where the coefficients a_0 and a_1 are:

$$
\begin{aligned}
a_0 &= G_{xx}\left(j\omega\right) G_{yy}\left(j\omega\right) \left(\alpha_{xx}\alpha_{yy} - \alpha_{xy}\alpha_{yx}\right) \\
a_1 &= \alpha_{xx} G_{xx}\left(j\omega\right) + \alpha_{yy} G_{yy}\left(j\omega\right)
\end{aligned}
\tag{11}
$$

The complex-valued eigenvalue Λ is related to the limiting depth of cut b_{lim} (above which chatter occurs) by:

$$
b_{\lim} = -\frac{2\pi}{N_t K_t} \operatorname{Im}\left(\Lambda\right) \left(\frac{\operatorname{Re}\left(\Lambda\right)}{\operatorname{Im}\left(\Lambda\right)} + \frac{\operatorname{Im}\left(\Lambda\right)}{\operatorname{Re}\left(\Lambda\right)} \right)
\tag{12}
$$

Meanwhile, the corresponding spindle speed is given by:

$$
\Omega = \frac{60\omega}{N_t \left(3\pi - 2\angle\Lambda + 2\pi n\right)} \quad n = 0, 1, 2, ..., N
\tag{13}
$$

where N is the maximum 'lobe number' that is in practice capped at a value of 10 or 20. At this stage it is worth pointing out that the solution of Eq. (12) and Eq. (13) involves solving a second order complex eigenvalue problem. Although this can be performed analytically, the outputs are not guaranteed to be monotonic with respect to the inputs. This has implications when a fuzzy arithmetic approach is applied.

2.3. Simplification for one-dimensional vibration

If the machine structure can be considered rigid in either the x or y directions, then G_{xx} or G_{yy} will be zero. Referring to Eq. (11), it can be seen that $a_0 = 0$, so Eq. (10) can be rewritten as:

$$
\Lambda = -\frac{1}{a_1}
\tag{14}
$$

8

Budak and Altintas [14] showed that the stability equations become similar to those for turning applications [1]:

$$b_{lim} = \frac{-1}{2N_t K_s Re\left(G_{OTF}\left(j\omega\right)\right)} \tag{15}$$

where $G_{OTF}(j\omega)$ is the *orientated transfer function*, i.e. the non-zero frequency response function (G_{xx} or G_{yy}) scaled by an orientation coefficient. The spindle speed is given by:

$$\Omega = \frac{60\omega}{2\pi N_t\left(n + \frac{\phi}{2\pi}\right)} \tag{16}$$

Here, ϕ is an angle based on the Nyquist diagram for the frequency response function $G_{OTF}(j\omega)$:

$$\phi = 2\pi - 2\text{atan2}\left(\text{Re}(G_{OTF}(j\omega)), \text{Im}(G_{OTF}(j\omega))\right) \tag{17}$$

2.4. TFEA chatter stability analysis

The preceding sections have shown that the milling chatter stability can be determined analytically, but the approach assumes that the periodic cutting force coefficients can be time-averaged. It transpires that this approximation becomes less accurate at lower radial immersions (r in Fig. 2). Although the time-averaged approach can be extended to account for this issue [15], the present study will apply a different approach [16] that uses temporal finite element analysis. Rather than averaging the time-periodic cutting force coefficients, this technique starts by writing the system equations of motion in the form:

$$\dot{\mathbf{y}}\left(t\right) = \mathbf{A}_t\left(t\right)\mathbf{y}\left(t\right) + \mathbf{B}_t\left(t\right)\mathbf{y}\left(t - \tau\right) \tag{18}$$

Where the time-periodic matrix coefficients $\mathbf{A}_t$ and $\mathbf{B}_t$ include the time-periodic cutting force coefficients and the state-space equations of motion for the structural dynamics. The stability of Eq. (18) is analysed by investigating the eigenvalues (characteristic multipliers) of the corresponding discrete map (mapping the state variables $\mathbf{y}$ from one tooth pass to the next). The discrete map is formed from two regions of the tool rotation. In the first region, no teeth are engaged in the workpiece, so the tool experiences free vibration, and the motion can be determined analytically. In the second case, when a tooth is engaged in the

9

workpiece, the time-finite element method is employed. An assumed solution for the state and delayed state are written as a linear combination of polynomials:

$$y\left(t\right) = \sum_{i=1}^{3} \mathbf{a}_{ji}^{n}\varphi_i\left(\sigma\right)$$
$$y\left(t - \tau\right) = \sum_{i=1}^{3} \mathbf{a}_{ji}^{n-1}\varphi_i\left(\sigma\right)$$
(19)

Here, σ represents the 'local time' within each temporal element j. Substituting these trial solutions into Eq. (18) leads to a non-zero error. The method of weighted residuals is then applied to each temporal element in turn. The results can then be assembled to produce an equation that relates the states of the system for the current tooth pass to those for the previous tooth pass:

$$\mathbf{y}_n = \mathbf{Q}\mathbf{y}_{n-1}$$
(20)

Finally, the eigenvalues of $\mathbf{Q}$ can be used to determine the chatter stability. Eigenvalues with magnitude less than unity indicate stable, chatter-free cutting.

Compared to the time-averaged method, the TFEA approach can provide a more accurate stability prediction because it accounts for the periodic terms in the cutting forces. This becomes increasingly important at low radial immersions, where each tooth is only engaged in the workpiece for a small proportion of its full rotation. It has been shown [17, 18] that this low radial immersion can give rise to period-doubling bifurcations in addition to the classical secondary Hopf bifurcations that are normally associated with milling chatter.

It is useful to point out that this stability analysis involves the numerical solution of a relatively low order (e.g. 16th order) eigenvalue problem. Although this can be done extremely quickly, for each spindle speed the computation must be repeated over a range of values of the depth of cut b. The stability boundary (i.e. stability lobe diagram) can then be determined by interpolation to estimate the combinations of b and Ω that result in marginal stability (i.e. an eigenvalue of unity). Again, the eigenvalue problem means that the outputs are not guaranteed to be monotonic with respect to the inputs.

3. Fuzzy arithmetic

Section 2 has summarised two techniques for predicting chatter stability. In this section, fuzzy arithmetic methods will be described, so that the stability analyses can be encoded with fuzzy input variables.

Fuzzy arithmetic has been used by various researchers as a technique for propagating uncertainty or variability through complex engineering models. The origins of this approach can be found in the theory of Fuzzy Sets. In contrast to classical set theory, the elements of a fuzzy set are assigned a degree of membership to the set, which is referred to as the membership level μ. The core of the set is defined as the subset of elements for which $\mu=1$, whilst the support is the subset for which $\mu>0$. A fuzzy number is a fuzzy set that is convex and normal, and whose membership function is piecewise continuous [7]. An example of a symmetric triangular fuzzy number is given in Fig. 4.

As the name implies, fuzzy arithmetic involves performing mathematical operations on fuzzy numbers, rather than conventional numbers. However, this can be a challenging problem, and so many researchers have resorted to approximating the fuzzy arithmetic processes by performing multiple evaluations at different membership levels. The resulting data is then used to approximate the output fuzzy number, by determining the maximum and minimum values for each membership level. For monotonic problems this process can become trivial, since the maxima and minima of the inputs will lead to the maxima or minima for the output. For non-monotonic problems (such as the chatter stability models developed in Section 2), this is no longer the case, and so alternative methods must be employed. This situation is further complicated when the arithmetic involves complex numbers. To tackle this problem, two alternative techniques are now described: complex interval-based arithmetic, and 'transformation methods'.

3.1. Interval-based arithmetic

Returning to Fig. 4, it can be seen that at membership level μ_j, the value of x can lie anywhere between $\underline{x_j}$ and $\overline{x_j}$. As previously mentioned, it is desirable to determine the associated range of values for some function $f(x)$. Interval analysis is one technique that can
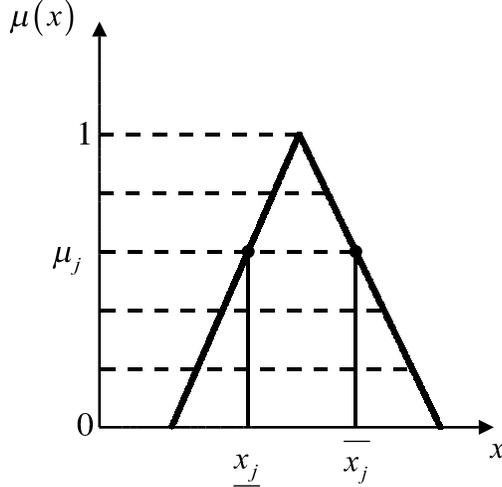
11

Figure 4: Representing a fuzzy number as an interval using α-cuts

be employed for this problem. Perhaps the most significant early work on interval arithmetic was its application to digital computing in the 1960's [19]. With interval arithmetic, the range of values of x is represented as an interval number, $[\underline{x_j}, \overline{x_j}]$. Arithmetical operations can then be defined for interval numbers. For example, interval addition and multiplication:

$$
[\underline{x_j}, \overline{x_j}] + [\underline{y_j}, \overline{y_j}] = [\underline{x_j} + \underline{y_j}, \overline{x_j} + \overline{y_j}]
$$
$$
\left[\underline{x_j}, \overline{x_j}\right] \times [\underline{y_j}, \overline{y_j}] = [\min\{\underline{x_j}\underline{y_j}, \underline{x_j}\overline{y_j}, \overline{x_j}\underline{y_j}, \overline{x_j}\overline{y_j}\}, \max\{\underline{x_j}\underline{y_j}, \underline{x_j}\overline{y_j}, \overline{x_j}\underline{y_j}, \overline{x_j}\overline{y_j}\}]
\tag{21}
$$

However, a major problem with interval arithmetic is the issue of dependency. A simple example demonstrates that interval arithmetic does not necessarily follow the law of distributivity, for three interval numbers $x = [0, 1], y = [-1, 2], z = [3, 4]$:

$$
x \times (y + z) = [0, 1] \times ([-1, 2] + [3, 4]) \qquad\qquad = [0, 1] \times [2, 6] \qquad = [0, 6] \tag{22}
$$
$$
(x \times y) + (x \times z) = ([0, 1] \times [-1, 2]) + ([0, 1] \times [3, 4]) \quad = [-1, 2] + [0, 4] \quad = [-1, 6] \tag{23}
$$

It can be seen that interval arithmetic is not capable of recognising multiple occurrences of the same variable, and evaluates each occurrence as being independent of the other. When an interval variable occurs more than once in an expression, large overestimation of the interval range can occur. This is demonstrated by Eq. (23) giving a range of [-1,6], instead of [0,6].

12

One solution to this problem is to attempt to track the dependency between variables, using the concept of affine arithmetic.

Affine arithmetic. Affine analysis attempts to allow for uncertainty in parameters whilst accounting for dependency between operands. Affine arithmetic provides a conservative solution set which is guaranteed to contain the true solution. The method is based upon work by Hansen [20], and was developed by Comba and Stolfi [21], whose main area of interest was computer graphics. More recently, it has been applied to some problems in structural dynamics by Manson [22], and this approach will be adopted for the present study. Since the chatter stability problem can involve complex numbers (e.g. frequency response functions), complex affine arithmetic will be used.

In general, an uncertain, possibly complex-valued parameter can be represented in a complex affine form as:

$$\hat{x} = x_0 + \sum_{i=1}^{n} x_i \varepsilon_i + x_{\text{real}} \varepsilon_{\text{real}_x} + i x_{\text{imag}} \varepsilon_{\text{imag}_x} \tag{24}$$

where x_0 is the central value of the parameter, x_i are partial deviations, and ε_i are real-valued symbolic variables that lie in the range [-1,1]. Each ε_i represents one of n sources of uncertainty, whilst the corresponding partial deviation gives the magnitude of that particular uncertainty. Some arithmetic operations on affine forms cannot be expressed without an approximation error; the real and imaginary values of the approximation error are accounted for by the (real-valued) terms x_{real} and x_{imag} respectively.

Manson [22] developed various complex affine operations (addition, subtraction, multiplication, division) which will be used in the present study. Earlier work [23] also developed approximations for unary non-affine operations on real affine forms. The procedure involved finding a 1st order polynomial approximation to the operation, and then including an additional error term such that the resulting affine form contained all possible solutions to the true solution:

$$\hat{y} = \alpha \hat{x} + \beta + \delta \varepsilon_{err_y} \tag{25}$$

This approach will be used in the present study to enable reciprocal, cosine, arc tangent, and 4-quadrant arc tangent operations on real affine forms.

13

Quadratic arithmetic. Manson, Chetwynd, and Worden [24] used the concept of quadratic arithmetic as a natural extension of affine arithmetic, for real-valued parameters. This method is similar to the Taylor arithmetic methods which are reviewed by Neumaier [25]. In the present study, the work of Manson [24] is extended by introducing the complex quadratic form of a parameter:

$$\hat{x} = x_0 + \sum_{i=1}^{n} x_i \varepsilon_i + \sum_{i=1}^{n} \sum_{j=i}^{n} x_{ij} \varepsilon_i \varepsilon_j + x_{\text{real}} \varepsilon_{\text{real}_x} + i x_{\text{imag}} \varepsilon_{\text{imag}_x} \tag{26}$$

The advantage of using complex quadratic arithmetic, compared to complex affine arithmetic, is that the second order interactions between the deviation terms can be accounted for when performing multiplication. Arithmetical operations based upon quadratic forms are derived in Appendix A, and further details on this approach are described in ref. [26].

In the present study, it is also necessary to perform continuous unary operations on real-valued quadratic forms. It transpires that this can be achieved using Eq. (25), in the same way as for affine forms. However, it should be noted that this approach has not directly made use of the 2nd order deviation terms, since only a linear approximation has been used.

A major drawback with the quadratic approach, compared to affine arithmetic, is that the range of the uncertain parameter cannot be readily determined. The quadratic deviation terms ($\varepsilon_i \varepsilon_j$ in Eq. (26)) mean that the minimum or maximum value of a parameter does not necessarily occur at extreme values of the uncertainties ε. This has implications for complex quadratic forms, since their set boundary is no longer a convex hull. Consequently, the solution set can only be represented by evaluating the parameter at selected values of the deviation coefficients, which together with an error term give rise to multiple convex hulls. Further details of these issues, along with some numerical examples, are given in ref. [22].

3.2. Application to chatter stability.

To demonstrate the application of affine and quadratic arithmetic to the problem of machining chatter, a numerical example will now be presented. The example considers a milling problem using the parameters given in Table 1, where two of the inputs involve

14

uncertainties that are intervals expressed in affine form. It should be pointed out that if the input uncertainties were fuzzy numbers then such intervals could be obtained by choosing an α-cut as illustrated in Fig. 4.

The machine tool structure consists of a single mode of vibration in the x direction, and the stability lobes can be calculated using Eq. (15) and Eq. (16). For the chosen parameters these equations can be re-written as follows:

$$\hat{b}_{lim} = \frac{-1}{2N_t K_s Re\left(\hat{G}_{OTF}\left(j\omega\right)\right)} \tag{27}$$

where $\hat{G}_{OTF}(j\omega)$ is the orientated transfer function in affine or quadratic form due to the uncertainty in the transfer function G_x and the cutting force angle β. The spindle speed is given by:

$$\hat{\Omega} = \frac{60\omega}{2\pi N_t \left(n + \frac{\hat{\phi}}{2\pi}\right)} \tag{28}$$

where $\hat{\phi}$ is the quadratic or affine form that arises due to the two input uncertainties. The predicted relationships between frequency, stability boundary, and spindle speed are shown in Fig. 5 for the case of quadratic arithmetic. The stability boundary now has a very large range, but this reflects the true range of the stability boundary (computed using thousands of samples across the interval range of the two inputs). However, the spindle speed prediction (Fig. 5(b)) for the quadratic arithmetic method becomes so wide that it becomes impossible to assemble a meaningful stability lobe diagram. The reasons behind this issue are illustrated in Fig. 6, which plots the real part of the frequency response function $G_{xx}(j\omega)$. Even if quadratic arithmetic is used, the prediction in the region of interest is relatively poor.

To recap, fuzzy arithmetic can in theory be performed by a series of interval arithmetic operations, for different membership levels (α-cuts) of the input fuzzy numbers. However, this simple example has demonstrated that even if the more advanced forms of interval arithmetic are used (affine and quadratic arithmetic), the predictions are over-conservative. In fact, the predicted interval ranges are so large that the methods become impractical for the milling chatter problem. Consequently, the remainder of this article will focus on alternative methods for performing fuzzy arithmetic, in particular the transformation method [4].

15

Parameter	Value
Number of teeth N_t	2
Radial immersion r/D (%)	50
Cutting stiffness K_s (N/m^2)	794x10^6
Cutting force angle $\hat{\beta}$ (deg)	$71.8 + 6\varepsilon_2$
k_x (N/m)	8x10^6
$\hat{m}_x$ (kg)	$0.2026 + 0.002\varepsilon_1$
c_x (Ns/m)	25.46
$\hat{G}_x(j\omega)$ (m/N)	$(k_x - \hat{m}_x\omega^2 + jc_x\omega)^{-1}$

Table 1: Parameters for affine arithmetic example. Uncertain inputs are given in affine form.
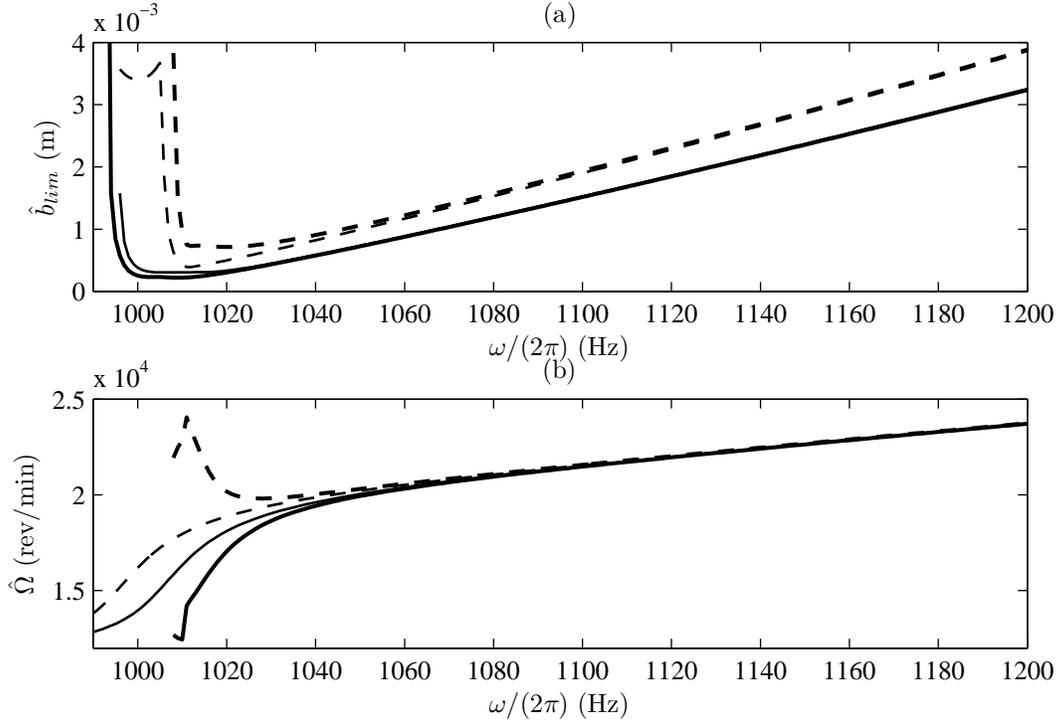

Figure 5: Stability boundary at different chatter frequencies. (a) depth of cut at the boundary of stability (b) spindle speed a at the boundary of stability. ▬▬▬ lower quadratic bound; ▬ ▬ ▬ upper quadratic bound; ▬▬ lower true bound; ▬ ▬ ▬ upper true bound.
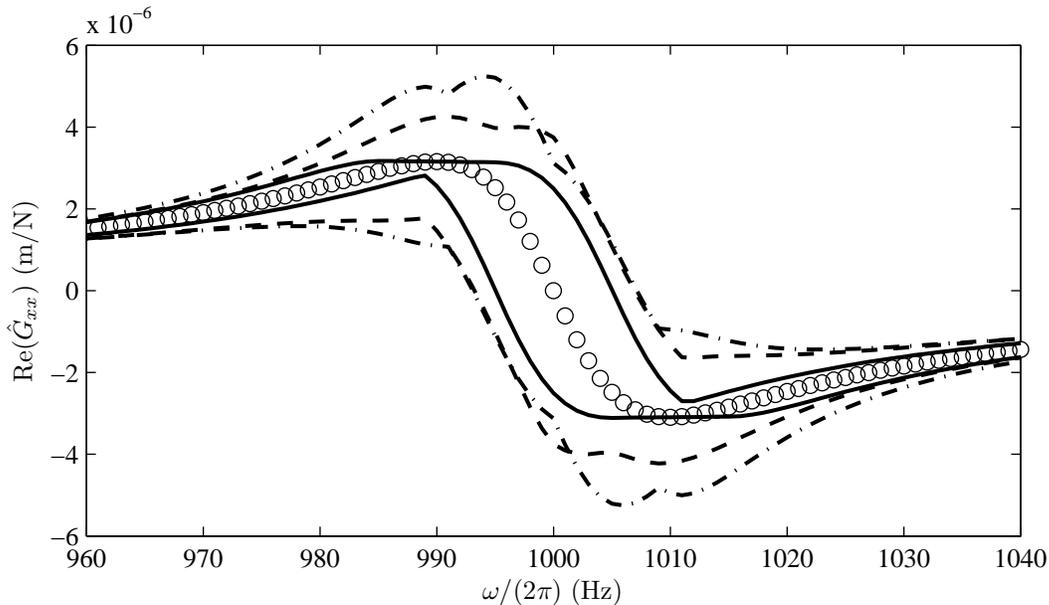
Figure 6: Real part of the x-direction FRF. ○ Crisp; —— True range. — — — quadratic range; —·—·— Affine range.

3.3. Transformation methods

Recall that the interval arithmetic techniques represented fuzzy numbers as intervals for each level of membership (or α-cut), as was shown in Fig. 4. An alternative approach is to perform a series of 'crisp' calculations using a sample of the possible values of each input 5 fuzzy number at that level of membership. The range of the output fuzzy number can then be approximated by determining the maxima and minima of the solution samples. Unlike the interval methods, this approach is not conservative, since the true maxima and minima are not guaranteed to coincide with the sampling points.

Perhaps the simplest method of choosing the necessary sampling points is the so-called 10 vertex method. This is illustrated in Fig. 7(a). However, this approach is unsuitable for problems involving 'extreme points' [27] (i.e. local maxima or minima) within the fuzzy values of the response. One solution is to perform multiple permutations for each level of membership (Fig. 7(b)), but some researchers have suggested more elaborate sampling techniques that can obtain similar results with fewer sampling points (and therefore reduced 15 computational cost).
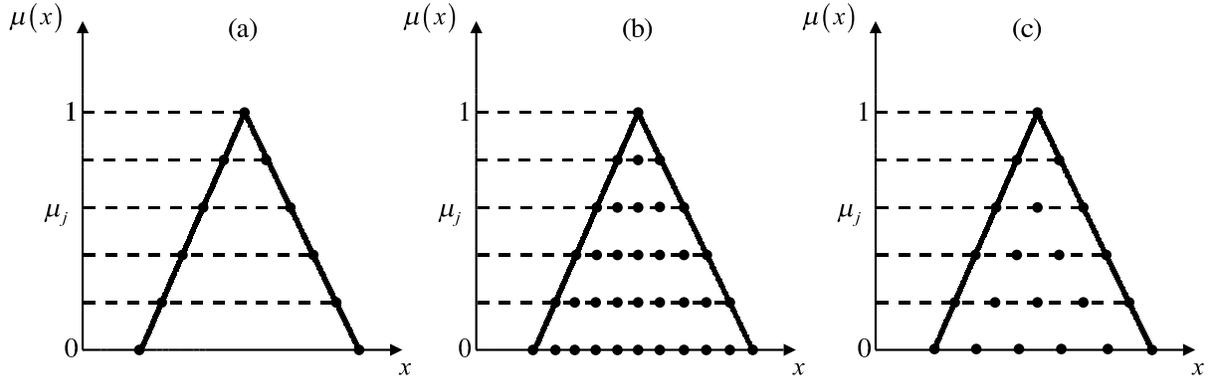
17

Figure 7: Fuzzy arithmetic performed using sampling methods. In the vertex method (a), samples are taken at the extreme values of each level of membership. A simple permutation method (b) includes the samples from higher levels of membership. In the transformation method (c), an alternating sequence of samples is obtained.

One such technique is the Transformation Method and its variants [8]. This is illustrated in Fig. 7(c). Rather than reproduce the details of this approach, the present article will illustrate its implementation using a simple example taken from [9]. Here, a polynomial test function with two fuzzy input parameters (x_1 and x_2) and one fuzzy output is evaluated. The inputs x_1 and x_2 are non-symmetric triangular fuzzy numbers, and the inputs and output are shown graphically in Fig. 8. In Fig. 9, the transformation method is compared to a vertex propagation technique for approximating the fuzzy output $f(x_1,x_2)$. In the vertex propagation approach, the range of each fuzzy number is determined at different levels of membership. The function evaluations are then performed for all of the permutations of these values. In the transformation method, a similar procedure is employed, but the odd and even membership levels are treated separately. This reduces the number of permutations required. Although the accuracy is also reduced, the alternating pattern means that the chosen parameter values are more evenly distributed within the multi-dimensional parameter space. This approach is described in detail by Klimke [9]. For the example problem shown in Fig. 8 and Fig. 9, it can be seen that adequate accuracy is achieved using 7 or 9 membership levels with the transformation method. Consequently, this methodology was adopted for the chatter stability problem.
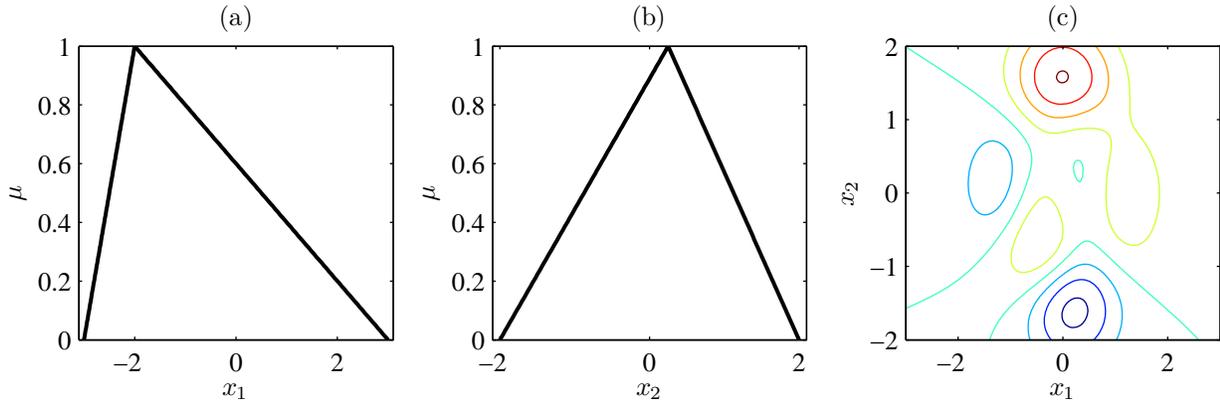
18

Figure 8: Input fuzzy numbers (a and b) and output contours (c) showing local maxima/minima of $f(x_1, x_2)$.

3.3.1. Implementation

In this section, implementation of the fuzzy stability lobe algorithms is described. However, it should be re-iterated that this approach involves performing multiple deterministic calculations based upon the relevant non-fuzzy stability equations (Eq. (12) and Eq. (13) for the time-averaged model, and determining the eigenvalues of **Q** in Eq. (20) for the TFEA model). Consequently, the approach is not concerned with the explicit fuzzy form of the stability equations. Instead, the numerical methods for implementation of the fuzzy stability lobe algorithms are described.

For the time-averaged stability model, it was shown in section 2.2 that the stability boundary can be computed using scalar arithmetic. For non-fuzzy problems, this code can be easily 'vectorised' to compute the stability over the N_ω values of ω found in the frequency response functions $G_{xx}(j\omega)$ and $G_{yy}(j\omega)$. Such an approach is highly desirable when using the array arithmetic capabilities of software such as Matlab. In this case, the function arguments and internal variables are either scalar quantities or vectors of size $[N_\omega$ x $1]$. The function outputs are a $[N_\omega$ x $1]$ vector of limiting depths of cut $\mathbf{b}_{lim}$, and a $[N_\omega$ x $N]$ matrix of spindle speeds Ω, where N is the maximum lobe number n used in the computation of Eq. (13) or Eq. (16). It is usually desirable to reduce these outputs to obtain a single stability lobe that is calculated at predetermined spindle speed values $\Omega_{desired}$. This can be achieved using 2 dimensional linear interpolation between the rows of data points in Ω, and
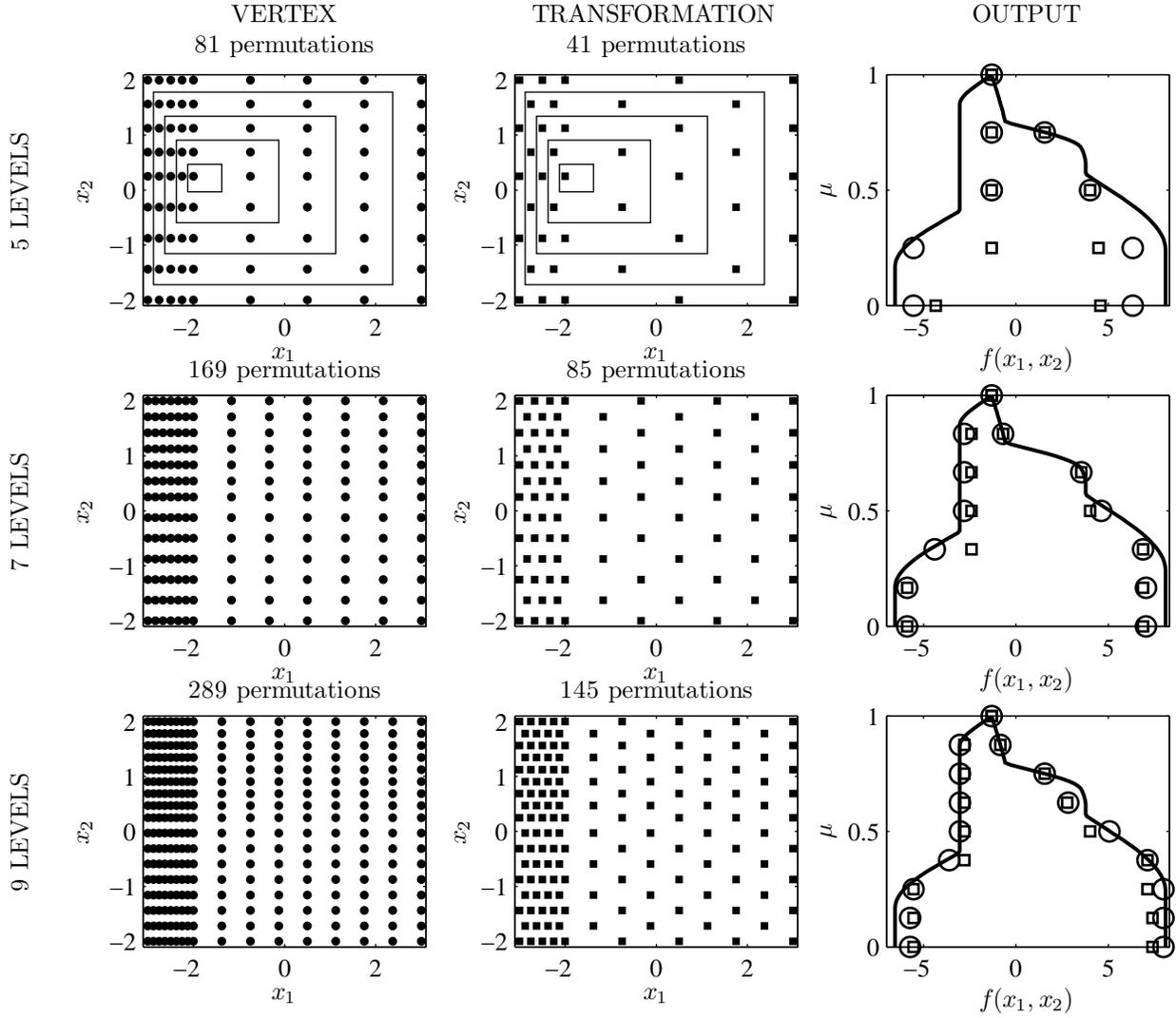
19

Figure 9: Comparison of a simple vertex method with an implementation of the transformation method. Column 3 compares the results with the true fuzzy output (■■■). The approximated value is shown as ◯ (vertex) or □ (transformation) markers. In row 1, the permutations used for each level of membership are shown by rectangular boxes.

20

the corresponding vector $\mathbf{b}_{lim}$. The minimum value is then selected from the columns (i.e. the lobe numbers) in each row, to obtain the final stability lobe.

In the general case of fuzzy stability lobes, this problem must be repeated p times, where p is the number of permutations obtained using the transformation method. However, the computational speed can be improved significantly if all of the permutations are computed together using array mathematics. Of the input parameters to this problem, the vector of desired spindle speeds $\Omega_{desired}$ and scalar number of lobes N will always be non-fuzzy. However, the tool entry and exit angles ϕ_{st} and ϕ_{ex} may be fuzzy scalars, depending upon the fuzziness of the radial immersion r. The cutting coefficients K_n, K_t (or K_s, β) may be fuzzy scalars, and the frequency response functions $G_{xx}(j\omega)$, $G_{yy}(j\omega)$ may be fuzzy arrays if the structural dynamics are fuzzy. Consequently, the transformation method codes provided by Klimke [9] were re-written to allow for arbitrary combinations of fuzzy and non-fuzzy scalars and vectors. A wrapper function was also used to allow the structural dynamics to be specified as fuzzy modal parameters rather than frequency response functions.

For the TFEA stability model, in the non-fuzzy case the eigenvalues of Eq. (20) must be determined for each value of the depth of cut and spindle speed. When performing the computations with Matlab, considerable speed improvements can again be achieved using array mathematics. Although the final eigenvalue cannot be solved analytically, the preliminary computations that populate the matrix $\mathbf{Q}$ are particularly cumbersome since they rely on the output from symbolic computation software. This component of the algorithm was re-coded using 5-dimensional array mathematics: 2 dimensions for the final matrix $\mathbf{Q}$, one for the array of spindle speeds, one for the array of depths of cut, and one for the array of temporal elements. The final eigenvalue problem was then computed within a sequence of three nested for loops. Finally, interpolation was used to find the limiting depth of cut, i.e. where the largest eigenvalue magnitude exceeded unity.

In the general case of fuzzy stability lobes, this problem must also be repeated p times, and it is again desirable to allow the input variables to be either fuzzy or non-fuzzy. However, there are already five dimensions used to populate the matrix $\mathbf{Q}$, and so using array mathematics to include the fuzzy parameters could cause significant performance problems

21

due to memory usage. Consequently, the fuzzy permutations were evaluated sequentially in this case.

To illustrate the performance of the fuzzy stability lobe approach, two numerical examples will now be presented.

4. Case studies

4.1. Robust design

This section uses the time-averaged stability approach to evaluate the chatter stability of a rigid tool and flexible workpiece with one mode of vibration in the x-direction and one in the y-direction. The stiffness of the x-direction mode is a fuzzy number – in practice this may represent the variability from one workpiece to the next (e.g. due to design variants or production tolerances), or it may be due to the physical removal of material from the workpiece during machining. The empirical cutting force magnitude K_s is assumed to be non-fuzzy, but the angle β is a fuzzy number. In practice this may represent lack of knowledge about this particular combination of tool and workpiece, or it may represent the variation in tool performance due to tool wear. The input parameters are summarised in Table 2. The goal of the fuzzy stability analysis is to choose a combination of depth of cut and spindle speed which gives the highest material removal rate M_{rr} within a predefined spindle speed range, despite the uncertainty/variability in the input parameters.

Using the transformation method with 9 membership levels required 145 permutations of the stability algorithm. The permutations were calculated concurrently using array mathematics to solve Eq. (12) and Eq. (13). The calculation was performed in approximately 40 seconds on a desktop pc, which suggests that the approach would be viable for industrial practitioners. The resulting fuzzy stability lobe is shown in Fig. 10. Here, only the lowest stability value is plotted for each level, since from a practitioner's perspective the upper stability limit is not relevant. It should be noted that very similar predictions can be obtained using the TFEA stability algorithm, but at considerable computational cost.

Fig. 10 clearly demonstrates that the shape of the fuzzy stability lobe does not completely mimic that of the non-fuzzy case (i.e. where μ=0). In particular, the regions of lowest

22

stability occurs over larger spindle speed ranges, and the regions with maximum stability also move. This has implications for the optimal choice of the machining parameters, in particular the depth of cut and spindle speed. If one had performed a non-fuzzy analysis (i.e. where $\mu=1$) alone, then a sensible choice may seem to be a spindle speed of 15200rev/min, and 12mm depth of cut. This would seem conservative since these parameters are located away from the stability limit, so the unidentified uncertainty or variation in the stability boundary might not cause instability. However, the fuzzy analysis allows for the maximum material removal rate to be determined for the stability boundary at each level of membership. These values are shown with the circular markers on Fig. 10. It can now be seen that if one accepts the full variation/uncertainty in the input parameters (i.e. $\mu=0$) a more prudent parameter choice would be 18000rev/min, 7mm.

This result can also be presented using the robustness curve approach described by Ben Haim [28]. In Fig. 11, the robustness curve is obtained by assuming that the membership level μ is inversely related to robustness, i.e. $\mu=1$ represents zero robustness, and $\mu=0$ represents maximum robustness. Meanwhile, the 'reward' is the material removal rate, which (from Eq. (1) and Eq. (2)) is proportional to $b_{lim}\Omega$. The highest reward is achieved with a spindle speed of 15000 rev/min, but this has zero robustness. As the required robustness is slowly increased, the highest reward is achieved with slightly higher spindle speeds. However, when the required robustness is increased so that $\mu < 0.5$, preference reversal occurs (i.e. an abrupt change in the optimum conditions), and the best choice of spindle speed is in the region of 18000 rev/min.

4.2. Theory vs experiment

This section uses the TFEA stability model to determine the chatter stability of a flexible tool. The milling parameters are given in Table 3, and (with the exception of the fuzzy parameters) the values are taken from ref. [29]. In this earlier work, detailed experimental data was presented and compared to different stability models. In the present article, the aim is to demonstrate how fuzzy stability lobe predictions could serve to justify differences between the experimental and model data. In other words, the stability lobe prediction

23

Parameter	Value
x-direction stiffness ($\mathrm{Nm^{-1}}$)	$11 \times 10^6 \rightarrow 14 \times 10^6$ (symmetric triangular fuzzy)
x-direction mass (kg)	0.2026
x-direction damping ($\mathrm{Nsm^{-1}}$)	25.46
y-direction stiffness ($\mathrm{Nm^{-1}}$)	4.4×10^6
y-direction mass (kg)	0.1245
y-direction damping ($\mathrm{Nsm^{-1}}$)	26.07
Cutting coefficient direction β (degrees)	$68 \rightarrow 76$ (symmetric triangular fuzzy)
Cutting coefficient ($\mathrm{Nm^{-2}}$)	625×10^6
Radial immersion (-)	50%
Milling mode	Up milling

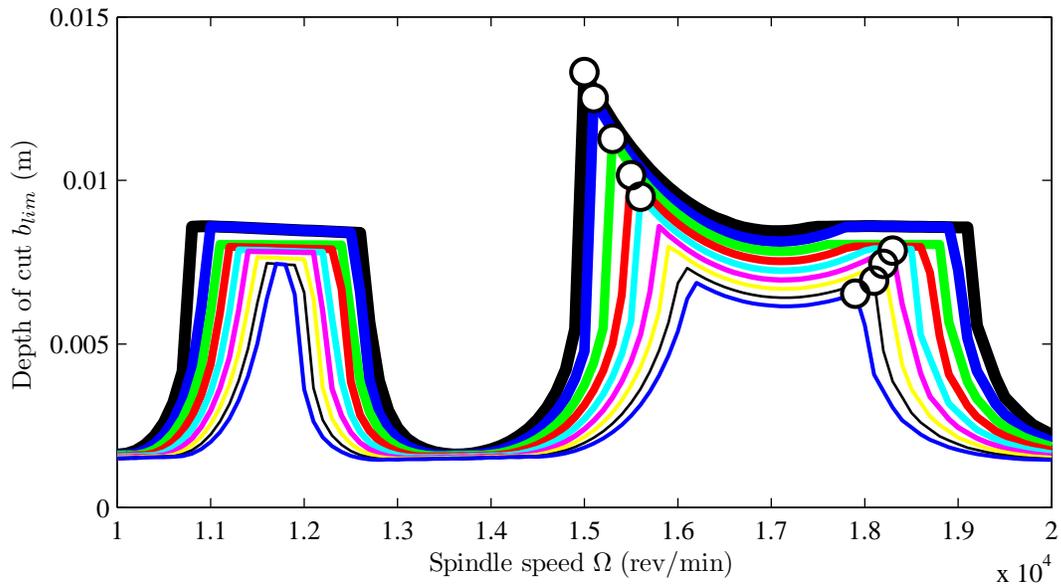Table 2: Parameters used for the 'robust design' case study.

Figure 10: Fuzzy stability boundary for example 1. ◯ Optimum —— $\mu = 0$, —— $\mu = 0.13$, —— $\mu = 0.25$, —— $\mu = 0.38$, —— $\mu = 0.5$, —— $\mu = 0.63$, —— $\mu = 0.75$, —— $\mu = 0.88$, —— $\mu = 1$.
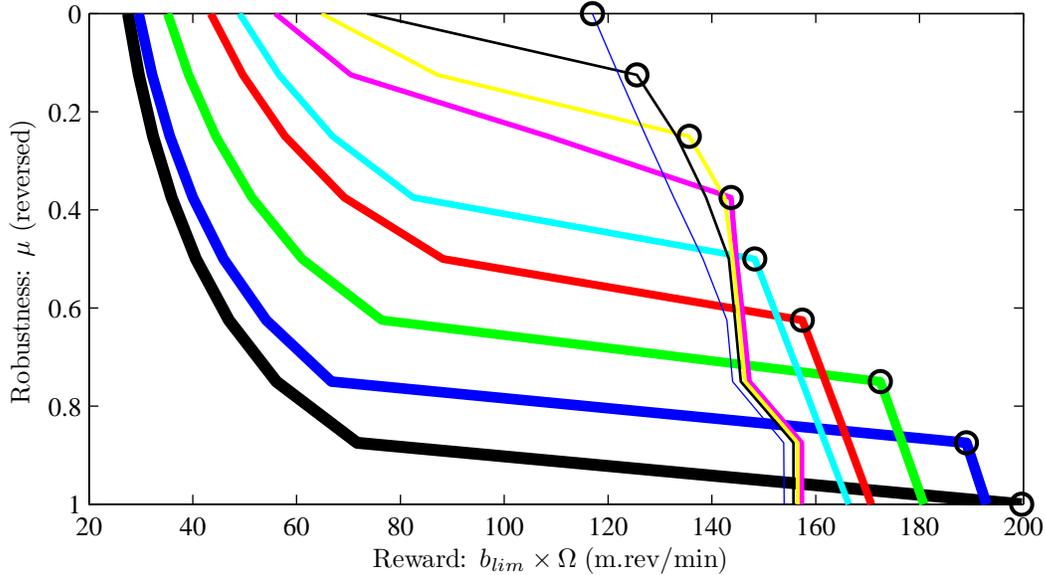
Figure 11: Robustness curve for example 1. ◯ Optimum ── 17900rev/min, ── 18100rev/min, ── 18200rev/min, ── 18300rev/min, ── 15600rev/min, ── 15500rev/min, ── 15300rev/min, ── 15100rev/min, ── 15000rev/min.

becomes a fuzzy prediction by accounting for parameter uncertainties, but no fuzzy analysis is performed on the experimentally obtained data.

As with the previous example, the empirical coefficient β is chosen to be fuzzy-valued to represent uncertainty or variation in the tool behaviour (due for example to tool wear). In addition, the radial immersion of the tool (as a percentage of its diameter) into the workpiece was given a fuzzy value. This was chosen because most stability models assume that the radial immersion matches the programmed value on the milling machine. In practice the deflection of the tool and workpiece mean that the actual radial immersion can be slightly different.

Using the fuzzy TFEA algorithm with 7 membership levels and two uncertain parameters resulted in 85 permutations, which were computed sequentially as previously described. In this case, the TFEA calculations took over 3 minutes on a desktop pc. If more membership levels were required, or more parameters were fuzzy, then substantially more computation time would be needed, making the approach unsuitable for use by industrial practitioners who may expect immediate analysis results.

In Fig. 12, the fuzzy stability boundaries for different membership levels are plotted. Because the aim here is to demonstrate how fuzzy stability lobes can justify the differences between theory and experiment, the upper boundary of the fuzzy stability lobe is also shown for each membership level. The experimental data obtained by Mann *et al* [29] is also shown as individual markers. For this scenario, the time-averaged stability model has not been used because it is unable to accurately predict the stability boundary for low-radial immersion milling.

For the non-fuzzy (μ=1) model, there are a few experimental data points that are close to the stability boundary but in disagreement with the model prediction. In Fig. 12(a), the cut at 2.5 mm, 17420 rev/min (shown with a double marker) should have been unstable according to the crisp stability lobe prediction, but was recorded as a stable case [29]. This data point lies within the fuzzy region of the stability lobe, indicating that the disagreement between theory and experiment could be accounted for by the uncertainty in the input parameters. The same issue applies for the experiment at 1.52 mm, 15050 rev/min (shown

Parameter	Value
x-direction stiffness (Nm^{-1})	1.666777×10^6
x-direction mass (kg)	0.061
x-direction damping (Nsm^{-1})	4.326
y-direction stiffness (Nm^{-1})	1.669223×10^6
y-direction mass (kg)	0.061
y-direction damping (Nsm^{-1})	3.858
Cutting coefficient direction β (degrees)	$69.6 \rightarrow 77.0$ (symmetric triangular fuzzy)
Cutting coefficient (Nm^{-2})	731×10^6
Radial immersion r/D (%)	$4.5 \rightarrow 5.5$ (symmetric triangular fuzzy)
Milling mode	Down milling

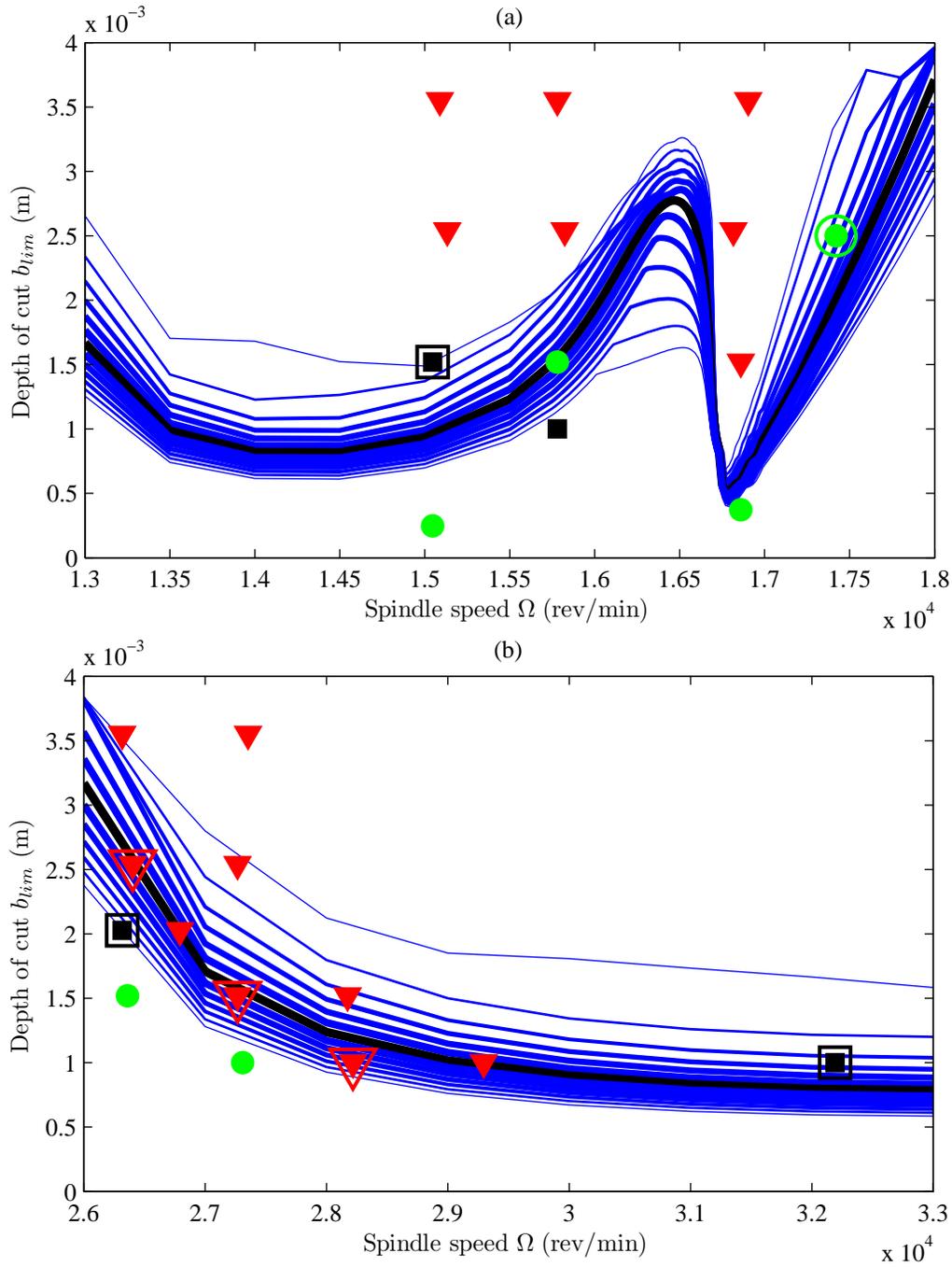Table 3: Parameters used for the 'theory vs. experiment' case study.

Figure 12: Fuzzy stability lobes for example 2. (a) Lower spindle speed range (b) higher spindle speed range. Experimental data: ■ borderline, ● stable, ▼ unstable. Fuzzy stability prediction: —— $\mu = 0$, —— $\mu = 0.17$, —— $\mu = 0.33$, —— $\mu = 0.5$, —— $\mu = 0.67$, —— $\mu = 0.83$, —— $\mu = 1$. Double markers indicate experimental outliers that are accounted for by the fuzzy analysis.

with a double marker). Here, the crisp stability prediction indicates that the experiment should have been unstable; the cut was actually 'borderline' (neither clearly stable nor clearly unstable) [29], and the discrepancy can be accounted for using the fuzzy stability lobes. Five similar scenarios arise in Fig. 12(b), and these are again shown with double markers.

To summarise, a number of the experimental outliers can be accounted for by a $\pm 5\%$ variation in the empirical value β, and a variation in the percentage radial immersion from 4.5% to 5.5%. However, it should be noted that there are some experimental data points that are not explained by this fuzziness (e.g. the 'borderline' case at 1 mm, 15780 rev/min). This suggests there is uncertainty/variability in the other parameters, or unmodelled behaviour.

5. Discussion

Before drawing conclusions, a number of issues are worthy of further discussion.

With regard to the interval arithmetic methods, we have shown that recursiveness makes them unsuitable for the chatter problem. Standard interval arithmetic was ruled out from the start: the simple numerical example of Eq. (23) demonstrated that the approach would vastly overestimate the interval bounds for each level of membership, if it were to be used in the fuzzy arithmetic. Although the affine and quadratic forms were shown to be more accurate, they still over-estimated the interval bounds when they were used for the simplest of milling chatter predictions. Although there are some potential improvements to these algorithms [21, 25], it seems unlikely that this would make them potential candidates for milling stability analysis.

Consequently, the remainder of this article focussed on 'design of experiments' approaches to performing fuzzy arithmetic. In particular, an implementation of the transformation method was developed by re-writing the code published by Klimke [9]. It has been shown here that for a simple stability analysis using the time-averaged model, the computational speed is sufficiently fast for quite a large number of model permutations to be performed interactively on a desktop pc. This suggests that more advanced methods for propagating uncertainty/variability may not be necessary. However, if detailed data were available on the statistical distributions of the input parameters, then a probabilistic analysis would be

28

more insightful than the fuzzy case. Although the chatter stability algorithms presented here would be amenable to Monte Carlo analyses, the higher numbers of simulation runs might cause problems. In this case, surrogate modelling techniques might prove useful.

The TFEA stability analysis was shown to have considerably higher computational time, suggesting that the fuzzy analysis may not be of benefit in an industrial scenario. Although more complex, the method is considerably more accurate for low-radial immersion milling, to the extent that the time-averaged method would give erroneous results if it were used for example 2 (Figure 8). Again, the possibility of detailed statistical data would mean that surrogate modelling approaches could be employed to provide probabilistic models of more uncertain scenarios.

It is worth noting that in implementing the Transformation Method, the user must decide upon the number of membership levels to be computed. In practice this is a trade-off between the accuracy of the result (compared to the true fuzzy number) and the computational effort required. In the present study 9 membership levels were used unless the computational effort was high, in which case 7 membership levels were used. This was shown (Figure 9) to be reasonably accurate even for very nonlinear problems.

One area in which the current results could be improved is the sensitivity analysis of the fuzzy stability lobes. Previous workers [14] have shown that the data used in the transformation method can be used to determine the sensitivity of the response to the different fuzzy inputs. Further work could investigate the application of this approach to the chatter stability problem.

6. Conclusions

The regenerative chatter stability of milling processes has been investigated using a fuzzy algorithm in order to accommodate uncertainty or variability in the model input parameters.

Implementations of complex affine and complex quadratic arithmetic were first developed, in an effort to perform fuzzy arithmetic based upon interval calculations at predetermined membership levels. However, it was shown using a simple machining example

29

that complex affine and complex quadratic arithmetic substantially over-estimate the chatter stability boundary, due to the problem of recursiveness.

A design of experiments approach to implement fuzzy arithmetic was then developed, using the algorithms proposed by Klimke [9]. It was shown that this formulation is well-suited to the chatter prediction problem, particular for the more straightforward time-averaged chatter model. Furthermore, it was demonstrated that this fuzzy approach can help to choose robustly optimal process parameters, and can also serve to justify the deviations between theoretical models and experimentally observed behaviour.

Acknowledgements

A. Quadratic arithmetic operations

For two complex quadratic forms $\hat{x}$ and $\hat{y}$, addition and subtraction are given by:

$$
\begin{aligned}
\hat{z} = \hat{x} \pm \hat{y} = x_0 \pm y_0 + \sum_{i=1}^{n} \left(x_i \pm y_i \right) \varepsilon_i + \sum_{i=1}^{n} \sum_{j=i}^{n} \left(x_{ij} \pm y_{ij} \right) \varepsilon_i \varepsilon_j \\
+ \left(x_{\text{real}} + y_{\text{real}} \right) \varepsilon_{\text{real}_z} + i \left(x_{\text{imag}} + y_{\text{imag}} \right) \varepsilon_{\text{imag}_z}
\end{aligned}
\tag{A.1}
$$

Multiplication by a complex scalar α is given by:

$$
\begin{aligned}
\hat{z} = \alpha \hat{y} = \alpha y_0 + \sum_{i=1}^{n} \alpha y_i \varepsilon_i + \sum_{i=1}^{n} \sum_{j=i}^{n} \alpha y_{ij} \varepsilon_i \varepsilon_j \\
+ \left(|\text{Re}\left(\alpha \right)| \, y_{\text{real}} + |\text{Im}\left(\alpha \right)| \, y_{\text{imag}} \right) \varepsilon_{\text{real}_y} \\
+ i \left(|\text{Re}\left(\alpha \right)| \, y_{\text{imag}} + |\text{Im}\left(\alpha \right)| \, y_{\text{real}} \right) \varepsilon_{\text{imag}_y}
\end{aligned}
\tag{A.2}
$$

Complex quadratic multiplication is rather more cumbersome:

$$
\begin{aligned}
\hat{z} = \hat{x} \times \hat{y} = \left(x_0 y_0 + \tfrac{1}{2} \sum_{i=1}^{n} \sum_{j=i}^{n} x_{ij} y_{ij} \right) + \sum_{i=1}^{n} \left(x_0 y_i + x_i y_0 \right) \varepsilon_i \\
+ \sum_{i=1}^{n} \sum_{j=i}^{n} \left(x_0 y_{ij} + x_{ij} y_0 \right) \varepsilon_i \varepsilon_j + \sum_{i=1}^{n} \sum_{j=1}^{n} x_i y_j \varepsilon_i \varepsilon_j + z_{\text{real}} \varepsilon_{\text{real}_z} + i z_{\text{imag}} \varepsilon_{\text{imag}_z}
\end{aligned}
\tag{A.3}
$$

where the real component z_{real} is:

$$
\begin{aligned}
z_{\mathrm{real}} = {} & \left(|\mathrm{Re}\,(x_0)| + \sum_{i=1}^{n} |\mathrm{Re}\,(x_i)| + \sum_{i=1}^{n}\sum_{j=i}^{n} |\mathrm{Re}\,(x_{ij})| + x_{\mathrm{real}} \right) \times y_{\mathrm{real}} \\
& + \left(|\mathrm{Im}\,(x_0)| + \sum_{i=1}^{n} |\mathrm{Im}\,(x_i)| + \sum_{i=1}^{n}\sum_{j=i}^{n} |\mathrm{Im}\,(x_{ij})| + x_{\mathrm{imag}} \right) \times y_{\mathrm{imag}} \\
& + x_{\mathrm{real}} \times \left(|\mathrm{Re}\,(y_0)| + \sum_{i=1}^{n} |\mathrm{Re}\,(y_i)| + \sum_{i=1}^{n}\sum_{j=i}^{n} |\mathrm{Re}\,(y_{ij})| \right) \\
& + x_{\mathrm{imag}} \times \left(|\mathrm{Im}\,(y_0)| + \sum_{i=1}^{n} |\mathrm{Im}\,(y_i)| + \sum_{i=1}^{n}\sum_{j=i}^{n} |\mathrm{Im}\,(y_{ij})| \right) \\
& + \sum_{i=1}^{n}\sum_{j=i}^{n}\sum_{k=1}^{n} |\mathrm{Re}\,(x_{ij}y_k + x_k y_{ij})| \\
& + \sum_{i=1}^{n}\sum_{j=i}^{n} |\mathrm{Re}\,(x_{ij})| \times \sum_{k=1}^{n}\sum_{l=k}^{n} |\mathrm{Re}\,(y_{kl})| - \tfrac{1}{2}\sum_{i=1}^{n}\sum_{j=i}^{n} |\mathrm{Re}\,(x_{ij})| \, |\mathrm{Re}\,(y_{ij})|
\end{aligned}
\tag{A.4}
$$

and the imaginary component z_{imag} is

$$
\begin{aligned}
z_{\mathrm{imag}} = {} & \left(|\mathrm{Re}\,(x_0)| + \sum_{i=1}^{n} |\mathrm{Re}\,(x_i)| + \sum_{i=1}^{n}\sum_{j=i}^{n} |\mathrm{Re}\,(x_{ij})| + x_{\mathrm{real}} \right) \times y_{\mathrm{imag}} \\
& + \left(|\mathrm{Im}\,(x_0)| + \sum_{i=1}^{n} |\mathrm{Im}\,(x_i)| + \sum_{i=1}^{n}\sum_{j=i}^{n} |\mathrm{Im}\,(x_{ij})| + x_{\mathrm{imag}} \right) \times y_{\mathrm{real}} \\
& + x_{\mathrm{imag}} \times \left(|\mathrm{Re}\,(y_0)| + \sum_{i=1}^{n} |\mathrm{Re}\,(y_i)| + \sum_{i=1}^{n}\sum_{j=i}^{n} |\mathrm{Re}\,(y_{ij})| \right) \\
& + x_{\mathrm{real}} \times \left(|\mathrm{Im}\,(y_0)| + \sum_{i=1}^{n} |\mathrm{Im}\,(y_i)| + \sum_{i=1}^{n}\sum_{j=i}^{n} |\mathrm{Im}\,(y_{ij})| \right) \\
& + \sum_{i=1}^{n}\sum_{j=i}^{n}\sum_{k=1}^{n} |\mathrm{Im}\,(x_{ij}y_k + x_k y_{ij})| \\
& + \sum_{i=1}^{n}\sum_{j=i}^{n} |\mathrm{Im}\,(x_{ij})| \times \sum_{k=1}^{n}\sum_{l=k}^{n} |\mathrm{Im}\,(y_{kl})| - \tfrac{1}{2}\sum_{i=1}^{n}\sum_{j=i}^{n} |\mathrm{Im}\,(x_{ij})| \, |\mathrm{Im}\,(y_{ij})|
\end{aligned}
\tag{A.5}
$$

References

[1] J. Tlusty, Manufacturing Processes and Equipment, Prentice Hall, New Jersey, 1999.

[2] G. S. Duncan, M. H. Kurdi, T. L. Schmitz, J. P. Snyder, Uncertainty propagation for selected analytical milling stability limit analyses, in: Transactions of the North American Manufacturing Research Institute of SME, Vol. 34 of 34th North American Manufacturing Research Conference, Milwaukee, WI, 2006, p. 17.

[3] H. De Gersem, D. Moens, W. Desmet, D. Vandepitte, A fuzzy finite element procedure for the calculation of uncertain frequency response functions of damped structures: Part 2 - numerical case studies, Journal of Sound and Vibration 288 (3) (2005) 463.

[4] M. Hanss, K. Willner, Fuzzy arithmetical modeling and simulation of vibrating structures with uncertain parameters, in: P. Sas, M. Munck (Eds.), Proceedings of the 2004 International Conference on Noise and Vibration Engineering, ISMA, Proceedings of the 2004 International Conference on Noise and Vibration Engineering, ISMA, Leuven, 2004, p. 3079.

[5] F. Kong, J. Yu, Study of fuzzy stochastic limited cutting width on chatter, The International Journal of Advanced Manufacturing Technology 33 (7) (2007) 677–683.

[6] K. Fansen, Y. Junyi, Z. Xiaoqin, Analysis of fuzzy dynamic characteristics of machine cutting process: fuzzy stability analysis in regenerative-type-chatter, International Journal of Machine Tools and Manufacture 39 (8) (1999) 1299–1309.

[7] S. Donders, D. Vandepitte, J. Van De Peer, W. Desmet, Assessment of uncertainty on structural dynamic responses with the short transformation method, Journal of Sound and Vibration 288 (3) (2005) 523.

[8] M. Hanss, The transformation method for the simulation and analysis of systems with uncertain parameters, Fuzzy Sets and Systems 130 (3) (2002) 277.

[9] A. Klimke, An efficient implementation of the transformation method of fuzzy arithmetic IANS Extended Preprint 2003/009.

[10] Y. Altintas, Manufacturing Automation: Metal Cutting Mechanics, Machine Tool Vibrations, and CNC Design, Cambridge University Press, 2000.

[11] M. Martellotti, An analysis of the milling process, Transactions of ASME 63 (1941) 677–700.

[12] M. Martellotti, An analysis of the milling process. part ii: down milling, Transactions of ASME 67 (1945) 233–251.

[13] E. Budak, Y. Altintas, Analytical prediction of chatter stability in milling - part i: general formulation, Journal of Dynamic Systems, Measurement and Control 120 (1998) 22–30.

[14] E. Budak, Y. Altintas, Analytical prediction of chatter stability in milling - part ii: application of the general forumulation to common milling systems, Journal of Dynamic Systems, Measurement and

Control 120 (1998) 31–36.

[15] S. D. Merdol, Y. Altintas, Multi frequency solution of chatter stability for low immersion milling, Journal of Manufacturing Science and Engineering, Transactions of the ASME 126 (3) (2004) 459–466.

[16] B. Patel, B. P. Mann, K. Young, Uncharted islands of chatter instability in milling, International Journal of Machine Tools and Manufacture 48 (1) (2008) 124–134.

[17] T. Insperger, B. P. Mann, G. Stepan, P. V. Bayly, Stability of up-milling and down-milling, part 1: alternative analytical methods, International Journal of Machine Tools and Manufacture 43 (1) (2003) 25–34.

[18] B. P. Mann, P. V. Bayly, M. A. Davies, J. E. Halley, Limit cycles, bifurcations, and accuracy of the milling process, Journal Of Sound And Vibration 277 (1-2) (2004) 31–48.

[19] R. Moore, Interval analysis, Prentice Hall, Englewood Cliffs, NJ, 1966.

[20] E. Hansen, A generalised interval arithmetic, in: N. K (Ed.), Interval mathematics, Vol. 29 of Lecture Notes in Computer Science, Springer-Verlag, 1975.

[21] J. Stolfi, J. Comba, Affine arithmetic and its applications to computer graphics, in: Proceedings of SIBRAPI93, Brazil, 1993.

[22] G. Manson, Calculating frequency response functions for uncertain systems using complex affine analysis, Journal of Sound and Vibration 288 (3) (2005) 487–521.

[23] G. Manson, Sharper eigenproblem estimates for uncertain multi degree-of-freedom systems, in: Proceedings of 21st International Modal Analysis Conference, Orlando, Florida., 2003.

[24] G. Manson, D. Chetwynd, K. Worden, Extending the prediction horizon of uncertain-weighted regression models, in: Proceedings of ISMA2006, Leuven, Belgium, 2006, pp. 1963–1974.

[25] A. Neumaier, Taylor formsuse and limits, Reliable Computing 9 (1) (2003) 43.

[26] N. Sims, G. Manson, Machining chatter: stability analysis using affine arithmetic, in: 1st International Conference on Uncertainty in Structural Dynamics, Sheffield, UK, 2007, pp. 365–376.

[27] W. Dong, H. C. Shah, Vertex method for computing functions of fuzzy variables, Fuzzy Sets and Systems 24 (1) (1987) 65–78.

[28] Y. Ben-Haim, Info-gap decision theory, Academic Press, Oxford, 2006.

[29] B. P. Mann, N. K. Garg, K. A. Young, A. M. Helvey, Milling bifurcations from structural asymmetry and nonlinear regeneration, Nonlinear Dynamics 42 (4) (2005) 319.